



Transport Measurements in Materials

A Major Qualifying Project
submitted to the Faculty of
Worcester Polytechnic Institute
in partial fulfillment of the requirements for the
Degree of Bachelor of Science

Submitted by:

Jeffrey P. Havill

Submitted to:

Project Advisors:

Professor Germano S. Iannacchione

Professor Diana A. Lados

July 3, 2014

This report represents the work of one or more WPI undergraduate students submitted to the faculty as evidence of completion of a degree requirement. WPI routinely publishes these reports on its website without editorial or peer review. For more information about the projects program at WPI, visit <http://www.wpi.edu/Academics/Projects>.

Abstract

The purpose of this experimental project was to design, construct, and validate a high-resolution apparatus to measure thermal and electrical property changes in heat treatable aluminum alloys. The materials chosen that make up the apparatus are determined by the desired properties for a 500 degree change that will isolate the sample material to give a one-directional thermal and electrical flow through the sample material. The goal was to measure these property changes caused from the development of precipitates forming due to artificial aging in-situ and ex-situ. Thermal resistance was measured at four different stages throughout the artificial aging process of wrought Aluminum 6061 and cast Aluminum 319 during a T6 temper. The design aimed to produce an apparatus that can be set up and swap sample materials with ease.

Acknowledgements

The author would like to profess their sincere appreciation for the effort and contributions to the following people:

The WPI Advisors:

Germano S. Iannacchione: Associate Professor and Department Head, Physics.

- Mr. Iannacchione was the heart of the project that had great ideas and information that went into this project every step of the way. Traits to note were his high energy levels and desire to help his students and would drop everything to answer my questions or give me tips for this project. Also, unlimited access to his equipment and machines in his laboratory, made the project run smoothly.

Diana A. Lados: Associate Professor, Mechanical Engineering. Affiliated with Aerospace engineering as well as Material Science and Engineering.

- Ms. Lados's extensive and widespread knowledge of multiple fields of engineering including aerospace, mechanical, and materials was much needed to direct the project. Her ability to link different fields of study efficiently is something to aspire for and was vital to keeping this project in up-to-date materials and uses in industry.

As well as Roger W. Steele, Anthony G. Spangenberg, and Xiang Chen who made this project possible.

Table of Contents

Abstract.....	ii
Acknowledgements.....	iii
List of Tables.....	vi
List of Figures	vi
1. Introduction.....	1
1.1 Overview.....	1
1.2 Project Objectives.....	2
1.3 Project Approach.....	2
2. Background.....	4
2.1 Literature Review.....	4
2.1.1 Thermal and Electrical Conductivity Measurements.....	4
2.1.2 Electrical transport.....	5
2.2 Fourier’s Law.....	6
2.3 Wiedemann-Franz Law.....	7
2.4 Heat Treating Aluminum Alloys.....	8
2.4.1 Precipitation Growth and Evolution.....	8
2.4.2 The Process of Heat Treatment.....	9
2.5 Aluminum 6061-T6.....	12
2.6 Aluminum 319-T6.....	13
3. Methodology	15
3.1 Design.....	15
3.1.1 Copper Connection Plates.....	17
3.1.2 Pyrex Tube.....	18
3.1.3 Copper-Brass Outer Canister.....	19
3.1.4 Teflon Spacers.....	19
3.1.5 Screw Assembly.....	20
3.2 Manufacture/Construction/Build.....	20
3.2.1 Copper Connection Plates.....	20
3.2.2 Teflon Spacers.....	21
3.2.3 Attachments to Connection Plates.....	21
3.3 Equipment/Machines used.....	22
3.3.1 Strain Gage Resistance Heater.....	22
3.3.2 Hi Speed USB Carrier.....	23
3.3.3 High Speed Power Supply.....	24
3.3.4 GE Varnish.....	24
3.4 Testing Samples.....	25
3.5 Validate/Calibration.....	26
3.5.1 Power	26
3.5.2 Thermocouple Calibration.....	27
3.6 Testing Technique.....	27
3.7 Analysis.....	28
4. Results and Discussion.....	32
5. Conclusions and Future Recommendations	34
6. Works Cited.....	35
Appendix A:	36

Appendix B.....	39
Appendix C.....	41

List of Tables.

Table 1: Aluminum alloy GP solvus temperature ranges (ASM).....	12
Table 2: Composition of Aluminum 6061 (ASM inc).....	12
Table 3: Aluminum 6061-T6 data (ASM inc).....	13
Table 4: Chemical composition of Aluminum 319.....	13
Table 5: Aluminum 319-T6 data (Granta).....	14
Table 6: Parameter Design Chart.....	16
Table 7: Properties of Silver, Copper, and Gold (Granta).....	17
Table 8: Aluminum samples heat treatment conditions.....	26

List of Figures.

Figure 1: Measurement device for thermal and electrical conductivity.....	4
Figure 2: Resistivity of Aluminum alloys at varying temperatures.....	6
Figure 3: Critical heating temperature from which quenching must take place during solution heat treatment.....	9
Figure 4: Aluminum temperature throughout heat treatment.....	10
Figure 5: Quench rate vs Yield strength in aluminum alloys.....	11
Figure 6: Section view of full apparatus (SolidWorks).....	15
Figure 7: Solidworks drawing of Copper Connection Plate.....	18
Figure 8: Solidworks drawing of Pyrex Tube.....	18
Figure 9: Solidworks drawing of Copper Canister.....	19
Figure 10: Solidworks Drawing of Teflon bottom.....	20

Figure 11: Strain gage.....	22
Figure 12: Strain gage information.....	23
Figure 13: National Instruments USB Carrier.....	23
Figure 14: High Speed Power Supply.....	24
Figure 15: GE #7031 Varnish.....	25
Figure 16: Temperature reading of hot and cold plate.....	28
Figure 17: Temperature difference between hot and cold plate.....	29
Figure 18: Raw temperature difference vs Raw Power applied.....	30
Figure 19: Calibrated temperature difference vs. calibrated Power.....	31
Figure 20: Aluminum 6061-T6 thermal resistivity vs artificial aging time length.....	32
Figure 21: Aluminum 319-T6 thermal resistivity vs artificial aging time length.....	33

1. Introduction

1.1 Overview

The concept of thermal conductivity allows for determination of the degree to which a specified material conducts heat. Materials of high thermal conductivity allow heat transfer to occur at a higher rate compared to materials with low thermal conductivity.

An accurate measurement of thermal conductivity is of importance in many applications from internal combustion engines and flying aircraft components to parts of computers. High thermal conductivity materials, mainly metals, are used at heat sinks in computers. This would dissipate heat quickly away from the central processing unit (CPU) in the computer, allowing the CPU to operate at a lower temperature. Low thermal conductivity materials can be used as heat shields to resist heat and keep it away from internal parts. Heat resistant tiles with very low thermal conductivity are used on the outside of Space Shuttles to keep the immense heat generated from friction away from the internal components. Also, very low thermal conductors are used as thermal barrier coatings for turbine blades to allow for higher service temperatures within the gas turbine.

In the present day, the concept and values of thermal conductivity of solid materials, on a larger than atomic scale, are well known. However, it took a while to fully grasp the idea of thermal transport within materials. “The concept of thermal conductivity required nearly three hundred years and involved the expenditure of an immense amount of mental energy and experimental effort. Galileo, Hooke, Newton, Boerhaave, Franklin, Black, Rumford, Fourier-giants in the scientific world-contributed to the development to this concept.[2]”

As the smaller distance you measure the heat transfer rate, or thermal conductivity, the more difficult it becomes. At the atomic or microscopic level it is hard to very accurate measure

the thermal conductivity or understand exactly how the heat is being transferred on this very small scale. With the increasing use of tempered alloys, the different phases within the material and how they affect thermal conductivity at the microscopic level is becoming more sought after.

1.2 Project Objectives

The main objectives of this MQP are to design, construct and validate a high resolution apparatus that measures the thermal conductivity of variable size materials. The apparatus would be able to measure thin pieces of material that are of low thermal conductivity as well as thick pieces of material that are of high thermal conductivity.

Once the apparatus is complete, a better knowledge of how different phases in heat treatable aluminum alloys affect thermal conductivity within the material is sought after. By studying the effects of different phases in those alloys, a better understanding of how the size and shape of precipitates within the aluminum affect thermal conductivity could be attained.

1.3 Project Approach

The design of the apparatus will be focused on creating a 1-dimensional flow of heat through the test samples. This is done by having the inside of the apparatus that surrounds the test samples have very low thermal conductivity. This will reject the heat and cause a more 1-dimensional flow through the test sample. The outside of the apparatus needs a material with a high heat capacity. This will create an environment within the apparatus where the temperature is negligibly affected by the outside temperature changes.

To study the effects of different microstructural changes within heat treatable alloys on thermal conductivity, two different aluminum alloys are tested. By looking at the thermal

conductivity at different stages of the heat treatment process as well as different alloying elements and phase structures, the effect on thermal conductivity can be examined.

2. Background

2.1 Literature Review

2.1.1 Thermal and Electrical Conductivity Measurements

Previous work has studied thermal and electrical conductivity measurements. “Thermal and electrical Conductivity Measurements of CDA 510 Phosphor Bronze,” written by J. Tuttle, E. Canavan, and M. Dipirro, who reported and determined varying electrical and thermal transport of different phosphor bronze formulations, where phosphor bronze’s electrical and thermal conductivity values have been published. The test apparatus used by Tuttle in which both the electrical resistivity and thermal conductivity measurements were performed is shown next in Figure 1.

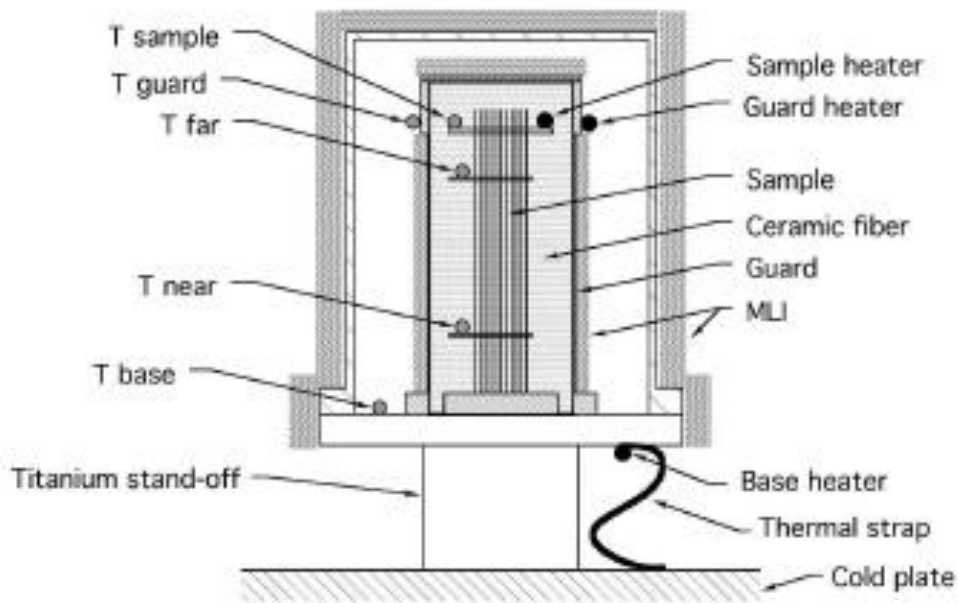


Figure 1: Measurement device for thermal and electrical conductivity.

The thermal conductivity measurement sample consisted of 10 parallel 76-mm-long phosphor

bronze wires with approximately 0.25 mm diameter. “A thin strip of 0.125-mm-thick copper ran perpendicular to the wires across their tops. This strip was soldered to each wire and served as the “sample-end” heat sink. A very small heater and CernoxTM thermometer were attached to this sink with GE varnish, with their leads extending upward.[5]”

Tuttle tested the electrical resistance of an 848 mm long sample of 0.249 mm diameter phosphor bronze CDA 510 wire. During this part of the experiment the base plate was controlled by temperature values between 4 and 300 kelvin. One of the results they determined was that the measured thermal conductivity and the electrical resistivity is not very well described by the Wiedemann-Franz law.

2.1.2 Electrical Transport

A Paper written by J. D. Jettomger “Electrical transport, thermal transport, and elastic properties of M_2AlC ($M=Ti, Cr, Nb, \text{ and } V$)” data was collected for good electrical and thermal conductors.

Different electrical resistivity with different Aluminum alloys was determined. Figure 2 shows an increase in electrical resistivity with higher temperatures:

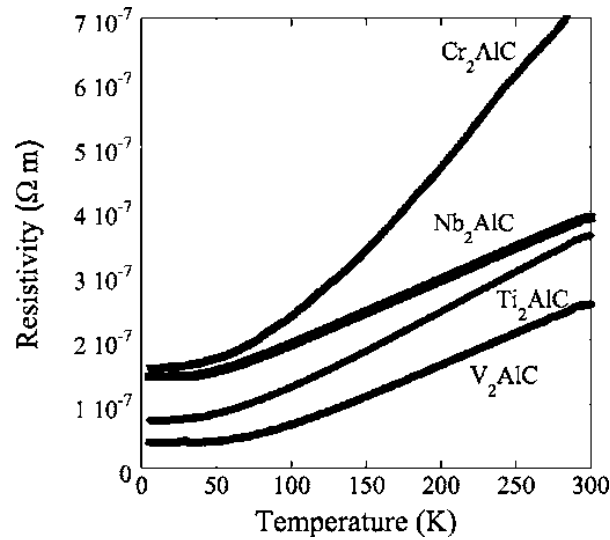


Figure 2: Resistivity of Aluminum alloys at varying temperatures.[6]

2.2 Fourier's Law

In determining the value of thermal conductivity for a material Fourier's law can be applied. This law is an empirical relationship between the conduction rate of heat in a material and the temperature gradient in the direction of energy flow.[7] The equation for a 1-directional heat conduction process can be expressed as:

$$q'_x = -\lambda dT/dx \quad \text{Equation (1)}$$

Where λ is the thermal conductivity constant (W/mK), q'_x is the heat flux (W/m²) in the positive x-direction, dT/dx is the negative temperature gradient (K/m) in the direction of heat flow. The heat flow due to conduction transfers from higher temperature to lower temperature resulting with the negative sign.

To get equation (1) in terms of thermal conductivity, it can be rearranged as:

$$\lambda = q'_x dx/dT$$

Where $q'_x = q/A$

$$\lambda = \frac{q dx}{A dT}$$

For this project the power q is determined from the heater used, the area A is area of the test samples, dx is the length of the test sample, and dT is the measured change from the power applied.

2.3 Wiedemann-Franz Law

The Wiedemann Franz law relates the thermal conductivity and the thermal conductivity in the equation:

$$\frac{\lambda}{\sigma} = LT \quad \text{Equation 2}$$

Where λ is thermal conductivity, σ is the electrical conductivity, T is the temperature, and L is the Lorenz number and is equal to $2.44 \times 10^{-8} \text{ [W}\Omega/\text{K}^2]$. [4]

This can be rearranged in terms of electrical conductivity expressed as:

$$\sigma = \lambda/(LT)$$

“Clearly there is a world of difference between the measurement of electrical conductivity and that of thermal conductivity. The relationship holds only for materials with more or less freely moving electrons; in other words, metals (at least at room temperature). [4]”

2.4 Heat Treating Aluminum Alloys

The goal of the treatment process is to increase the alloys' mechanical properties by precipitation hardening. This can lead to higher strength, stress-corrosion resistance, as well as easier to weld or extrude. According to the American Society for Metals (ASM) there are two prerequisites for a heat-treatable alloy to be considered age or precipitation hardening. The first having solid solubility of major alloying elements shall decrease with decreasing temperature. Then the second having Guinier-Preston (GP) zones solvus shall be sufficiently high to be able to form GP zones in a reasonable time. This says that there must be enough added elements in the aluminum to be available to form precipitates within the aluminum and not dissolve back into the aluminum after the process.

2.4.1 Precipitation growth and evolution

The GP zones are alloying elements that diffuse to form coherent precipitate clusters. These strengthening precipitates in an alloy are fine particles of an impurity phase. These impurities can lead to enhanced mechanical properties. The changes in the size of the precipitate can likely affect the thermal and electrical properties of aluminum. Precipitate sizes in alloys are a result from different aging conditions. The formation and growth of precipitates in an alloy can increase strength by impeding the movement of dislocations. In Figure 3 below, you can see the precipitates forming in the aging stage:

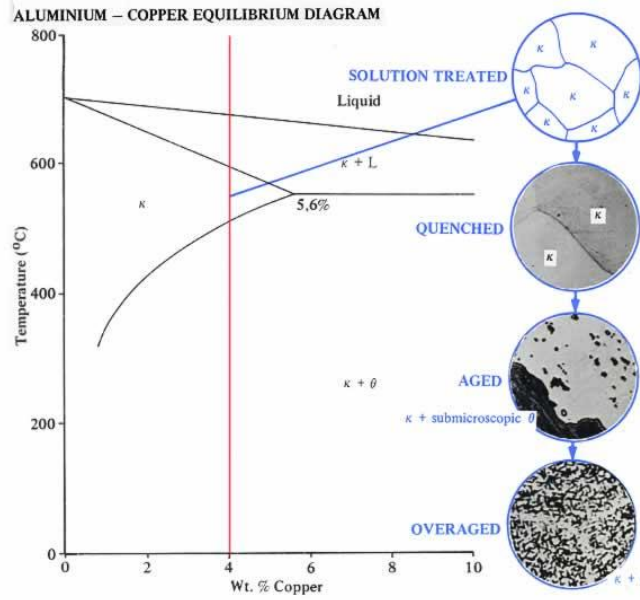


Figure 3: Critical heating temperature from which quenching must take place during solution heat treatment. [8]

2.4.2 The Process of Heat Treatment

Heat treating is a time-temperature process with or without cold working. This process includes three important steps; solution treatment, quenching, and ageing. Choosing different solution heat treatment temperature, quench rate, and aging practice are key features in getting enhanced properties. The relative temperature throughout the heat treatment process can be seen below in Figure 4:

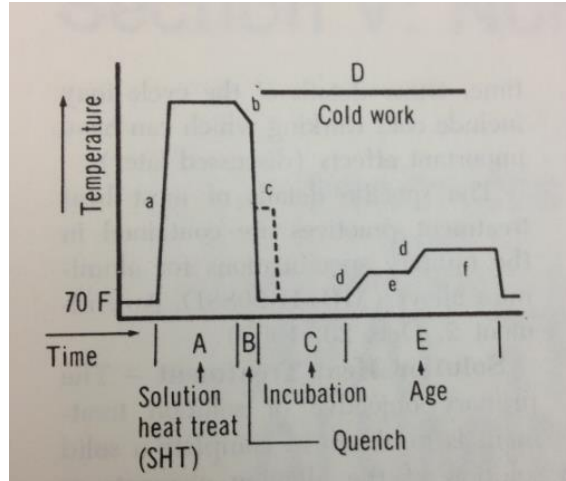


Figure 4: Aluminum temperature throughout heat treatment.[ASM]

Step 1: Solution Heat Treatment

The goal of solution heat treatment is to obtain as complete a solid solution of the alloying elements in the matrix as possible. The desire of this first step is to solutionize all the atoms in the aluminum alloy. This is done by heating up the aluminum alloy close to its melting temperature. In this process the high temperature is held constant from anywhere between 1-24 hours for the solution heat treatment.

Step 2: Quenching

After the solution heat treatment, quenching is required to retain both the solid solution and a sufficient supersaturation of vacancies for effecting aging. It is the rapid cooling of a material and attempts to maintain the crystalline structure or phase distribution that would be lost upon slow cooling. This is usually done by immersion in oil or water directly after the solution heat treatment. In this experiment the alloys will be quenched with boiling water. Mechanical properties are generally improved by specifying the fastest possible quench rate. However, for different properties such as stress-corrosion resistance, a slow quench rate is beneficial. In Figure

5 below, the effects of quench rate on yield strength of various aluminum alloys after aging to T6 temper.

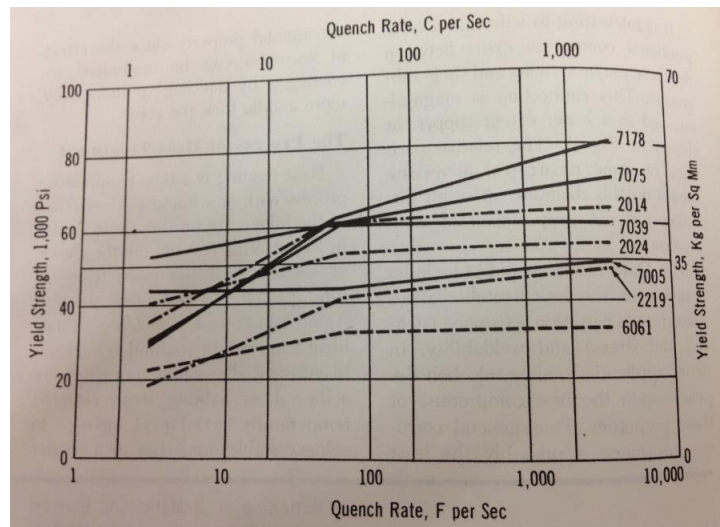


Figure 5: Quench Rate vs. Yield Strength in Aluminum alloys.[ASM]

Step 3: Aging

In the process of aging, the alloying elements within the aluminum starting forming together and make precipitates. These sough after precipitates are the reason for enhanced physical properties. Artificial aging is the process where the aluminum is reheated to increase the rate of precipitate formation. Whereas natural aging occurs at room temperate and precipitates form naturally.

Isothermal aging can be done up to the GP zone solvus as long as the heating rate is not too rapid. To go above the GP zone solvus a slow heating rate is required. In Table 1 below, approximated ranges for GP zone solvus of the main systems are given:

Table 1: Aluminum alloy GP zone solvus temperature ranges (ASM).

Aluminum	GP zone solvus temperature range
2000 series	350 to 410 F
6000 series	350 to 425 F
7000 series	230 to 325 F

Mostly, the highest mechanical properties are achieved at the lowest practical aging temperature. A higher aging temperature would be suitable for a spring and stress-corrosion resistance can be improved by higher aging temperatures or overaging. Overaging uses temperatures above the GP zone solvus.

2.5 Aluminum 6061-T6

Al 6061-T6 is widely used in many fields of industry including automotive and aerospace. This alloy is composed largely of Aluminum, Magnesium, silicon, and copper. The percentages can be found from the Aerospace Specification Metals Inc. in Table 2 below:

Table 2: Composition of Aluminum 6061.[1]

Component Wt. %		Component Wt. %		Component Wt. %	
Al	95.8 - 98.6	Mg	0.8 - 1.2	Si	0.4 - 0.8
Cr	0.04 - 0.35	Mn	Max 0.15	Ti	Max 0.15
Cu	0.15 - 0.4	Other, each	Max 0.05	Zn	Max 0.25
Fe	Max 0.7	Other, total	Max 0.15		

Data values for various properties relative to this experiment are shown below:

Table 3: Aluminum 6061-T6 Data. [1]

Property	Value
Electrical Resistivity	3.99e-006 ohm-cm
Thermal Conductivity	167 W/m-K
Melting Point	582 - 652 °C
Solution Temperature	529 °C
Aging Temperature	177 °C

2.6 Aluminum 319-T6

Al 319-T6 is commonly used in the automotive industry as a material for engine blocks and cylinder heads. This alloy is composed largely of Aluminum, Silicon, Magnesium, Copper and Iron.

Table 4: Chemical composition of Al 319.

Alloy type	Average composition, wt %										
	Si	Cu	Fe	Mg	Mn	Zn	Ti	Sr	Ni	Sn	Pb
319	7.70	3.38	0.38	0.27	0.23	0.08	0.12	0.0007	0.018	0.0033	0.012

Some data values for Al 319-T6 relevant to this experiment are shown below in Table 5 from Granta:

Table 5: Aluminum 319-T6 Data.[9]

Property	Value
Thermal Conductivity	109 [W/(m*k)]
electrical Conductivity	6.4E6 [ohm*cm]
Solution Temperature	502-507 Celsius for 8 hr
Aging Temperature	152-157 Celsius for 2-5 hr

3. Methodology

3.1 Design

Figure 6 shows the design of the apparatus in SolidWorks. The apparatus contains two end-caps, a hollow cylindrical outer body, and an inner cylindrical body to house the sample and the data collection instruments. The inner tube has to be a fairly good insulator such that the thermal conductivity experiment will not be affected; the preferred material for the inner tube will be quartz crystal. Quartz [Silicon Dioxide] is an electrical insulator with very low dielectric losses. Its insulating and dielectric properties are maintained over a wide temperature range. However Pyrex was used because of the availability with similar properties of Quartz. The outer cylindrical tube has to be a good conductor, thus copper would work well.

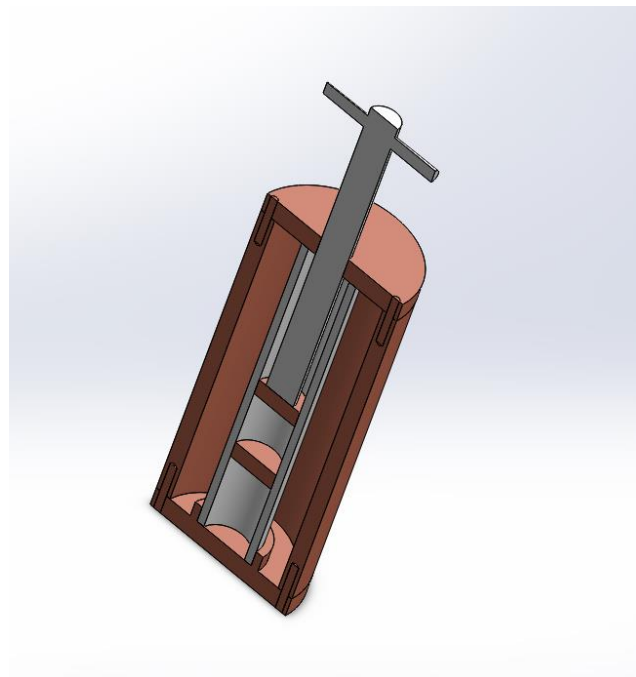


Figure 6: Section view of full apparatus (SolidWorks).

The end caps will also be made of copper but with modifications. There will be wires

coming out of the apparatus and a way of securing the sample inside the inner tube that will be directed through the end-caps. There has been a discussion as to what the wires should be made of and the conclusion was made to use copper wires due to their availability, they had the needed properties and they were cost effective.

Table 6: Parameter design chart.

Surface Area (A)	fixed value		
length (l)	variable value		
material selection:			
Contact Plates:	copper	small and highly electrical and thermal conductive.	
Contact Plates thickness	fixed value	unknown stiffness of compound	
Wire Connectors:	copper		
wire length:	short as physically possible	High electrical conductivity materials. i.e. silver, copper, gold, aluminum.	
tube/apparatus shell	glass	stiff/thick plastic compound	
sample geometry	cubic	cylindrical	
sample size	1" to 2" squared	1 to 2" diameter	
sample thickness	variable value		
Insulators	rubber or glass	dissipates heat and is not a conductor of electricity preferably.	
Design for apparatus closing	Spring loaded plate	Screw adjustment system	Push in cap

After putting the apparatus together, it has to be calibrated. This means that some experiments have to be done and based on the real values of a well-known pure element or alloy, it has to be calibrated around those values. In order to make any measurements, there has to be a way to get data and use a formula to get another set of data that are important. The project is to be computerized, meaning that a computer will be programmed to collect data and store them in a file that can be used to perform calculations. Automating this process will enable repeatable results and a very reliable method of data collection.

The goal of the design specifications were to make an apparatus that would have a high heat inertia so that when heat is added to a side of a sample, the change of temperatures of the

materials around the sample would be a negligible amount. Also, an important part of the design was to make something that is durable enough to handle a 500 degree Celsius change.

3.1.1 Copper Connecting Plates

This design includes two connection plates lightly clamping a sample material to measure thermal and electrical conductivity of that sample. Sought properties of the connection plates include the ability to conduct electricity and heat very well. Copper has a very low electrical resistivity and a high thermal conductivity. Copper will have really small voltage loss as well as minimal heat loss across the connection plates.

Table 7: Properties of Silver, Copper, and Gold.[9]

Material	Thermal Conductivity (W/(m*C))	Electrical resistivity (uohm*cm)	Melting point (Celsius)	Specific heat Capacity (J/(kg*C))	Tensile strength (MPa)	Compressive Strength (MPa)	Price (\$/gram)
Silver	415	1.6	960	235	150	55	1.06
Copper	395	1.93	1080	385	150	33	.0093
Gold	315	2.5	1065	130	200	190	58

The connection plates must be small and thin enough to come close to 1-directional heat and electrical flow and be rigid enough to not bend or warp. The diameter of the plate is 19.05mm the thickness is 2.54mm which is about the size of a penny. The thickness was selected to be thin enough that there would not be a temperature gradient across the connection plate that will be heated during experiment. The heated connection plate will ideally be completed uniform in temperature throughout the thin plate. The cross-sectional area of the connection plate was selected based on the size of the sample materials to be tested. A sample material of around a diameter of 19.05mm shows good results for finding thermal and electrical properties.

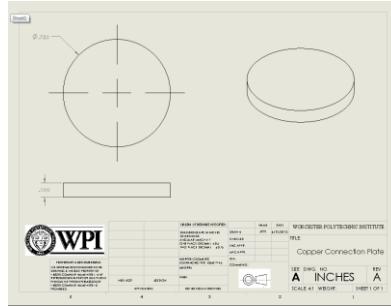


Figure 7: SolidWorks drawing of Copper Connection Plate.

The flatness of the connection plates come into play when heat transfer is occurring between the connection plates and sample material. Loss of heat transfer can occur if the contact surfaces between the connection plates and sample material are not smooth and flat. The contact sides of the connection plates are needed to be sanded and polished to a near perfect smoothness and flatness. The near perfect smoothness of the copper connection plates will make a more accurate thermal property reading. For the electrical property readings roughness does not come into play as long as there is a contact point.

3.1.2 Pyrex Tube

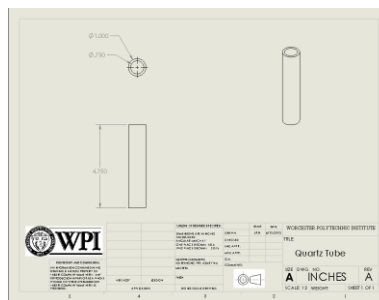


Figure 8: SolidWorks drawing of Pyrex Tube.

To make the experiment have as close to a 1-direction flow of heat and voltage, an insulator is needed to be around the connection plates and sample material. Quartz Tubing has a very high electrical resistivity along with a low thermal conductivity. Quartz will reject a lot of

heat and a lot of voltage, keeping the flow of heat and voltage 1-directional from the heated connection plate through the sample material and through the second connection plate. The quartz tube is 12.06cm tall. It has an ID of 19.05mm and OD of 25.4mm.

3.1.3 Copper-Brass Outer Canister

The Pyrex tube is going to be held in a wider copper cylinder with a copper lid and bottom. The Copper Canister will create high heat inertia for the whole apparatus. Copper has a high heat capacity meaning that it will be stubborn to change temperature compared to other materials. So once the whole apparatus is at a certain temperature, small heat fluxes will cause negligible temperature differences. This will give a more accurate thermal property reading when testing.

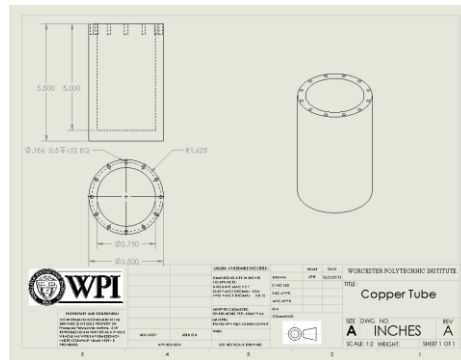


Figure 9: SolidWorks drawing of Copper Canister.

3.1.4 Teflon Spacers

To minimize heat loss through contact between the connection plates and other parts, Teflon is used. Teflon, Like Quartz, has a very low thermal conductivity. Using a Teflon spacer to hold up the bottom connection plate allows to minimize contact points of different parts to take heat away from the connection plates. A Teflon cap used between the contact points of the

Teflon screw, used to lightly hold the sample material between the two connection plates, and the top connection plate. This reduces the contact area from the Teflon screw to the smaller area of the Teflon cap. The Teflon cap which is in contact only with the perimeter of the cold connection plate, allows for a thermal couple placement directly in the middle of the connection plate which is in line with the thermal couple placed in the middle of the hot connection plate.

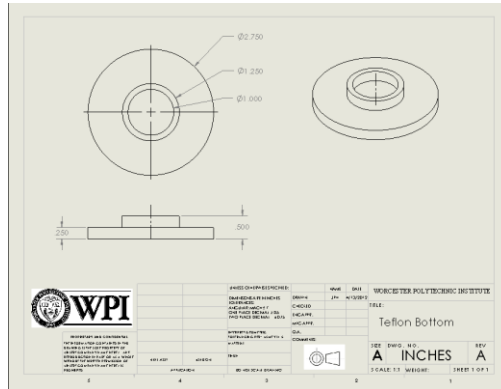


Figure 10: SolidWorks drawing of Teflon bottom.

3.1.5 Screw assembly

To hold the testing samples firmly between the two copper connection plates a screw assembly was used. This allows to lightly clamp the cold copper connection plate down onto the testing sample and hot copper connection plate. By twisting the screw it will push down on the cold copper connection plate. The material chosen for the screw was Teflon. The very low thermal conductivity of Teflon allowed for minimal heat leak from the sample to through the screw.

3.2 Manufacture/Construction/Build

3.2.1 Copper connection plates

The two copper connection plates were machine off a pure copper rod with a lathe. To achieve a very flat surface to improve thermal contact, sandpaper and polishers were used.

Starting with fine and ending with super fine grit grades of sandpaper were applied to achieve a mirror finish. The grades of sandpaper used were 400, 600, then 1200. After those three were applied the copper connection plates were then brought to a chemical polishing machine that was had velvet paper rated at 3,000 grade.

3.2.2 Teflon Spacers

The Teflon spacers were machine used a lathe. The inner diameter was slowly cut away at until the Pyrex tube fit snug, but not too tight to allow for thermal expansion.

The bottom Teflon spacer had a $\frac{1}{4}$ inch diameter hole drilled through the side to allow for the wires from the heater, electrical lead, and thermal couple to come out from the bottom of the hot copper connection plate.

The top Teflon spacer two $\frac{1}{4}$ inch diameter holes drilled. One was drilled in the side to allow the wires from the hot copper plate come out of the apparatus. The second was drilled in the top to allow the wires from the cold copper connection plate to come through the Teflon spacer and out of the apparatus with the wires from the hot copper connection plate. The top Teflon spacer also had a $\frac{1}{4}$ -20 screw thread tapped into the top to allow for the screw assembly to lightly clamp the testing samples in between the copper connection plates.

3.2.3 Attachments to connection plates

On the hot copper connection plate located at the bottom of the apparatus there is the resistance heater, thermocouple and electrical lead attached on the underside of the hot copper plate. The strain gage resistance heater was attached using a thin layer GE varnish. Then two thin wires were soldered onto each end of the heater to apply power to it. The thermal couple was

then placed directly on top and in the middle of the heater and held in place with more GE varnish. The electrical lead was soldered directly on the copper connection plate with some GE varnish for added strength because the solder onto copper was not very secure by itself.

On the cold copper connection plate located at the top of the apparatus there was a thermal couple and electrical lead attached to the top side of the cold copper plate. The thermal couple was attached directly in the middle of the copper plate and secured with GE varnish. The electrical lead was soldered directly onto the copper plate with some GE varnish on top for added strength.

3.3 Equipment/Machines Used

3.3.1 Strain Gage Resistance Heater

To apply heat to one side of our testing samples, a strain gage was used. By applying voltage to the strain gage, the resistance will cause it to heat up. This particular strain gage was chosen based on its circular dimensions. The hot copper connection plate it is attached to is circular and are both similar sizes making the temperature of the plate heat up evenly throughout.



Figure 11: Strain Gage



Figure 12: Strain Gage information

3.3.2 Hi Speed USB Carrier

To get the temperature readings from the two thermocouples to the computer a national instrument USB-9162 was used. This product includes LabVIEW Signal Express LE data-logging software which was the program used in the experiments to record temperature readings.

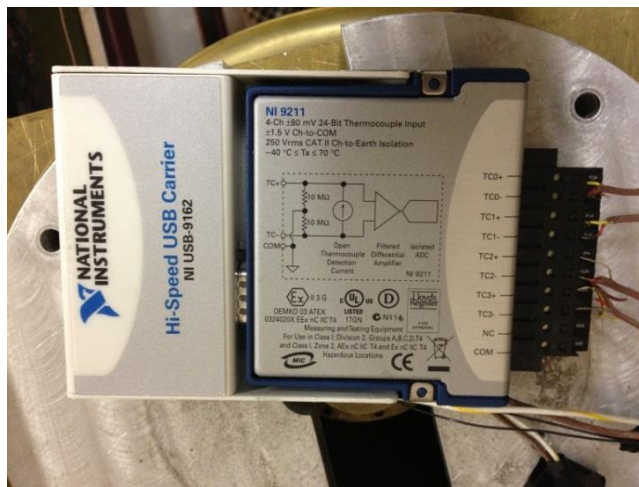


Figure 13: National Instruments USB Carrier

3.3.3 High Speed Power Supply

To send voltage to the resistance heater a Keithley 2304a DC Power Supply was used. This model provides both voltage control and power consumption monitoring for automated testing. These power supplies have outstanding voltage stability during pulse load changes and can simultaneously measure load currents.



Figure 14: High Speed Power Supply.

3.3.4 GE Varnish

The attachments to the hot and cold copper connection plates were glued and secured with GE #7031 adhesive and insulating varnish.

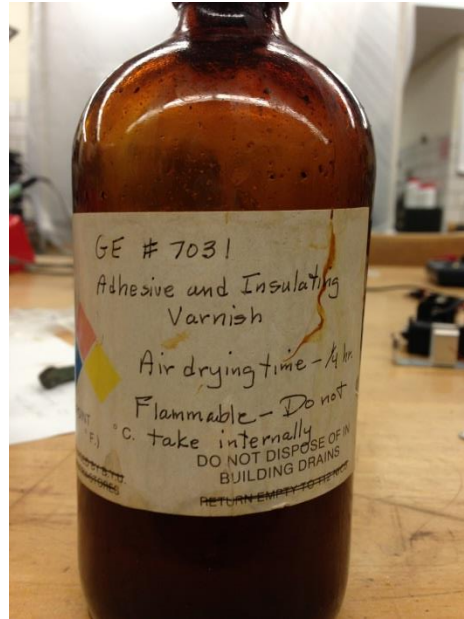


Figure 15: GE #7031 Varnish

3.4 Testing Samples

In this experiment there are 10 aluminum samples. Five samples are aluminum 6061 and five samples are aluminum 319. One of each aluminum alloy was let untouched by heat treatment and is called “initial conditions.” Then the other four samples from each aluminum alloy were solution heat treated and quenched. Once they were solution heat treated and quenched the thermal resistivity was measured on all ten of the aluminum alloy samples in the apparatus. Then, three samples of each aluminum alloy from the solution heat treated and quenched group were artificially aged at different time intervals. Then the thermal resistivity was measured again. From this, information on differences in thermal resistivity and aging time length is sought. The aluminum 319 is a cast alloy and the aluminum 6061 is wrought. This might also be an explanation for differences in thermal resistivity as aging time is increased. Values for the heat treatment process can be seen in the following table:

Table 8: Aluminum samples heat treatment conditions.

Testing Conditions					
Aluminum Alloy	Solution heat treatment		Quench	Artificial Aging	
	Temperature [°C]	Time [hours]		Temperature [°C]	Time [hours]
<i>Al-6061</i>					
Sample 10	Initial Conditions			Initial Conditions	
Sample 9	529	10	Warm Water	none	
Sample 6	529	10	Warm Water	180	Ex-situ: 4
Sample 7	529	10	Warm Water	180	Ex-situ: 8
Sample 8	529	10	Warm Water	180	Ex-Situ:16
<i>Al-319</i>					
Sample 5	Initial Conditions			Initial Conditions	
Sample 4	505	10	Warm Water	none	
Sample 1	505	10	Warm Water	180	Ex-Situ: 2
Sample 2	505	10	Warm Water	180	Ex-Situ: 4
Sample 3	505	10	Warm Water	180	Ex-Situ: 8

3.5 Validate/Calibration

3.5.1 Power

To determine the amount of power that actually propagates through the test samples, a calibration sample is needed. The calibration sample must have a well-know value for the thermal conductivity. The calibration sample used was pure copper. The value for the thermal conductivity of copper is known and widely accepted.

To method in determine the amount of power that goes into the sample for this apparatus, a fractional coefficient, c is determined. This calculated coefficient c , with take a fraction of the total power generated from the heater and give the amount of power that reaches the test samples. The process of determining the fractional coefficient c , can be seen from the work done in excel as follows:

<u>Thermal Conductivity of copper:</u> Thermal conductivity of copper @ room temp = 386 [W/K*m] $R_{cu} = 386 \text{ W/K*m}$
--

Dimensions of Cu Sample:

length:	2.40625	inches	0.06111875	meters
diameter:	0.625	inches	0.015875	meters

Conductance:

$$K = k_{Cu} * A_{Cu} / L_{Cu} = 1.250058077 \text{ W/K}$$

Resistance:

$$R = 1/K = 0.799962833 \text{ K/W}$$

Power Calculations:

$$P_T = dT/R_{Cu} \quad \text{Where } P_T \text{ is the total power through the sample.}$$

$$P_T = c * P_0 \quad \text{Fractional amount of the total power } P_0 \text{ leaked out}$$

Where P_0 is the total power generated by the heater.

$$c = (dT/P_0) * (1/R_{Cu})$$

$$c = 2.28/0.8$$

$$c = \mathbf{2.85}$$

3.5.2 Thermocouple calibration

Seeing how the thermocouples were not perfectly matching and the cold thermocouple was a little higher temperature than the hot thermocouple at room temperature, the temperature difference at zero power and room temperature was added to each DT_{raw} to determine DT_{corr}.

3.6 Testing Technique

- 1) The inner structure is set up by having a sample placed into the Pyrex tube and enclosed by the Teflon spacers. The copper connection plates are lightly clamping the sample by the Teflon screw.

- 2) The inner structure is then placed into the outer canister, then the out canister is placed into a dry tank.
- 3) Once the thermocouple readings are at equilibrium with the room temperature data was started to be logged.
- 4) The voltage to the strain gage heater was applied at 2 volts. Once the two thermocouples equilibrate with the heat addition, the voltage was increase to 4 volts, then 6 volts, then 8 volts.

3.7 Analysis

During the testing, values for the temperature of the hot and cold side of the test samples are recorded from the two thermocouples to the Hi-speed USB carrier to the computer using labVIEW. From this the hot and cold side of the test samples temperature data was measured. An example can graph can be seen below:

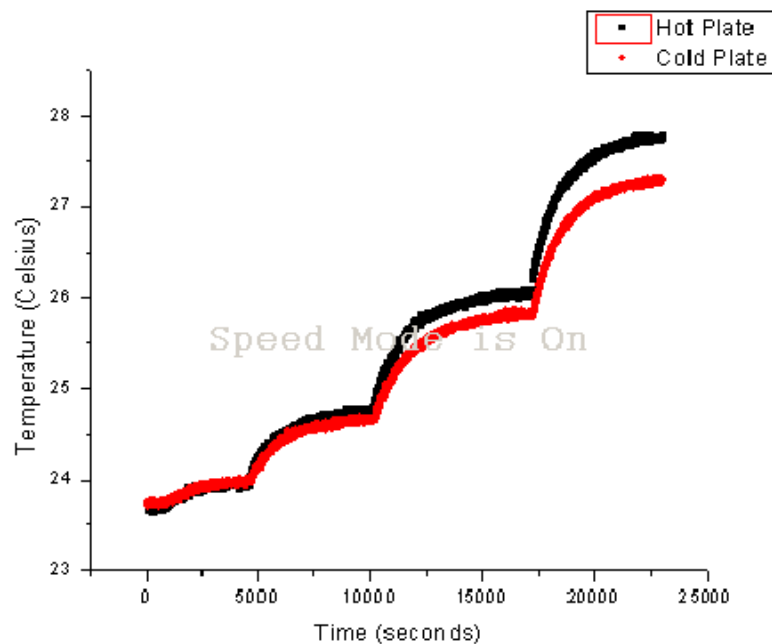


Figure 16: Temperature readings of hot and cold plate.

From the previous graph you can see the four temperature rises from the four different voltage increase to the heater. The temperature difference of the hot and cold plate can be seen and the difference gets larger as more heat is applied.

By subtracting the cold side temperature from the hot side temperature, the change in temperature can be determined. In the next graph, the temperature difference of the hot and cold side can be seen:

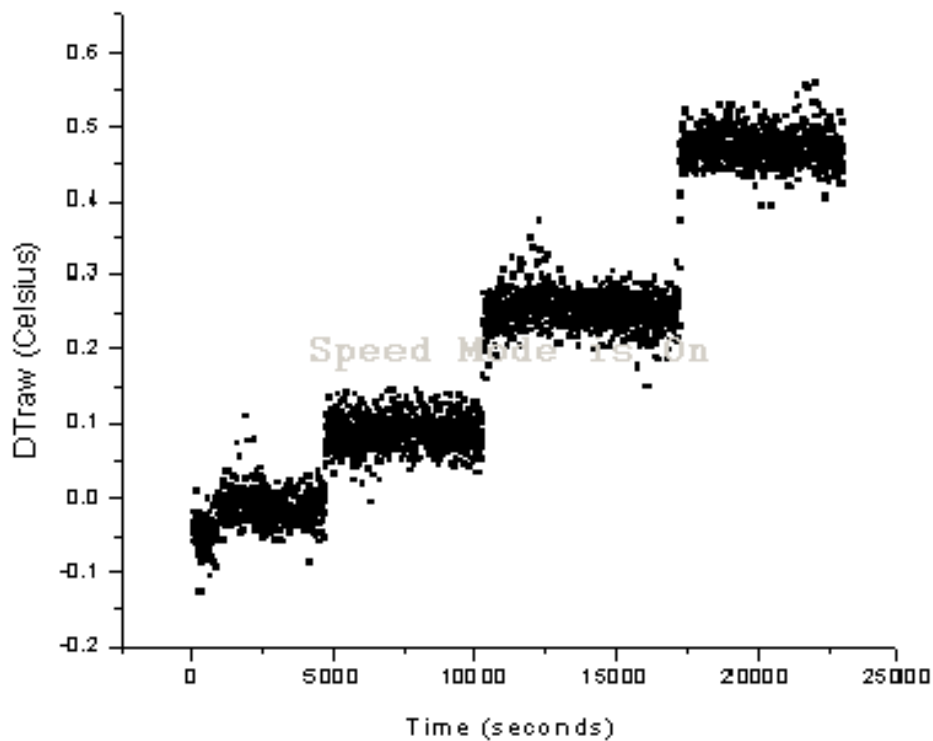


Figure 17: Temperature difference between hot and cold plate.

The four voltage increases to the heater can be clearly seen from the jumps to the higher temperature differences.

To get a single value for the difference in temperature of the two sides at each power level, the data point when the temperature rise has level off at each stage was averaged. With the thousands of data points at each power level, a good estimate and standard deviation for the

temperature difference was achieved. The average change in temperature of the hot and cold side at each power level can be seen in the following graph:

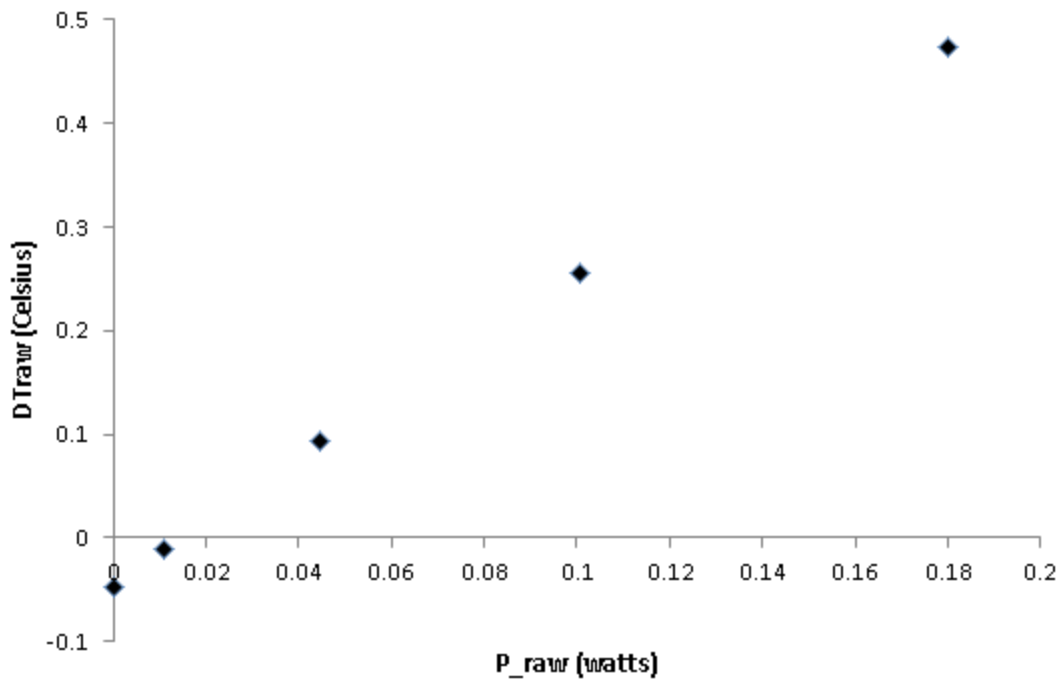


Figure 18: Raw temperature difference vs Raw Power applied.

The graph above shows five points starting from zero power applied. DTrawr in the above graph is the data as collected from the thermocouple and P_raw was the total power applied to the heater.

The data from the graph above in Figure 18 is the raw data that was taken directly from the thermocouple and power applied to the heater. In the graph below in Figure 19 it shows the data after being corrected and calibrated to a copper sample with known thermal conductivity. The process for calibration can be seen in section 3.5 validate/calibration.

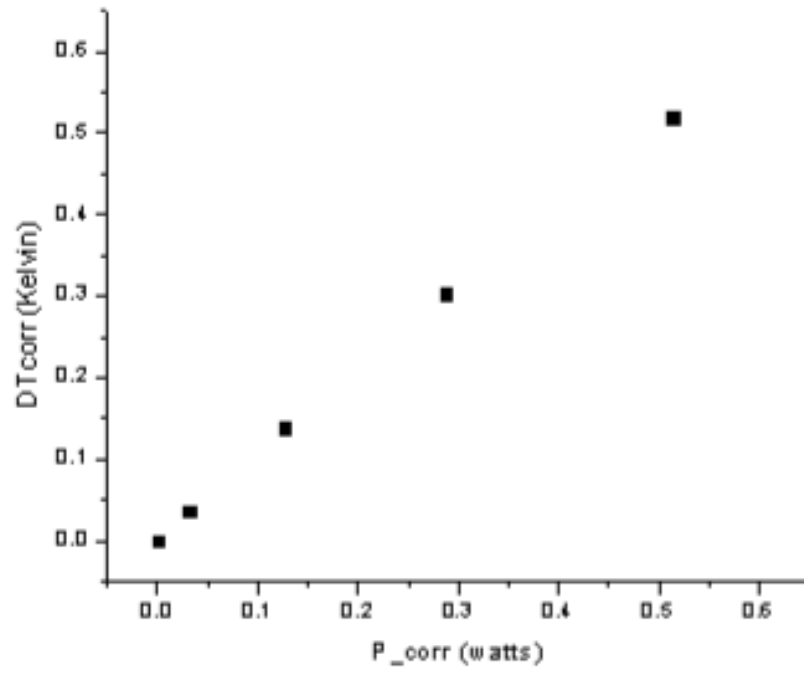


Figure 19: Calibrated temperature difference vs Calibrated Power.

4. Results and Discussions

It can be seen in both graphs in this section that at zero artificial aging time, the thermal resistance is lower. Then it seems to increase in thermal resistance in the earlier stage of artificial aging. At about half the time length for a T6 temper the thermal resistances decreases. At the full artificial aging time length for a T6 temper for both, aluminum 6061 and aluminum 319, the thermal resistance is at its highest.

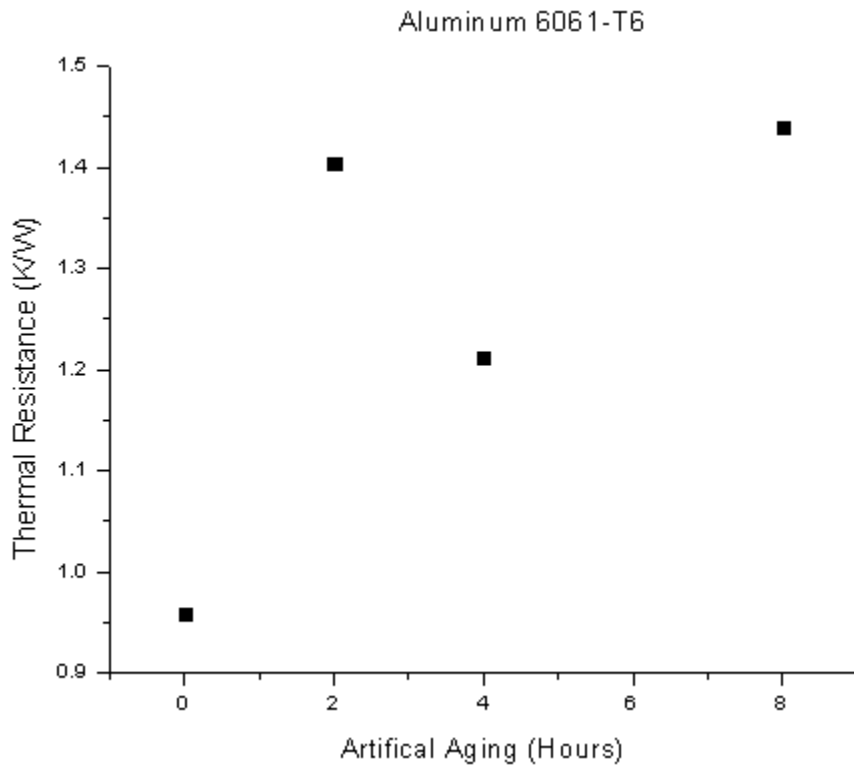


Figure 20: Aluminum 606-T6 thermal resistivity vs artificial aging time length.

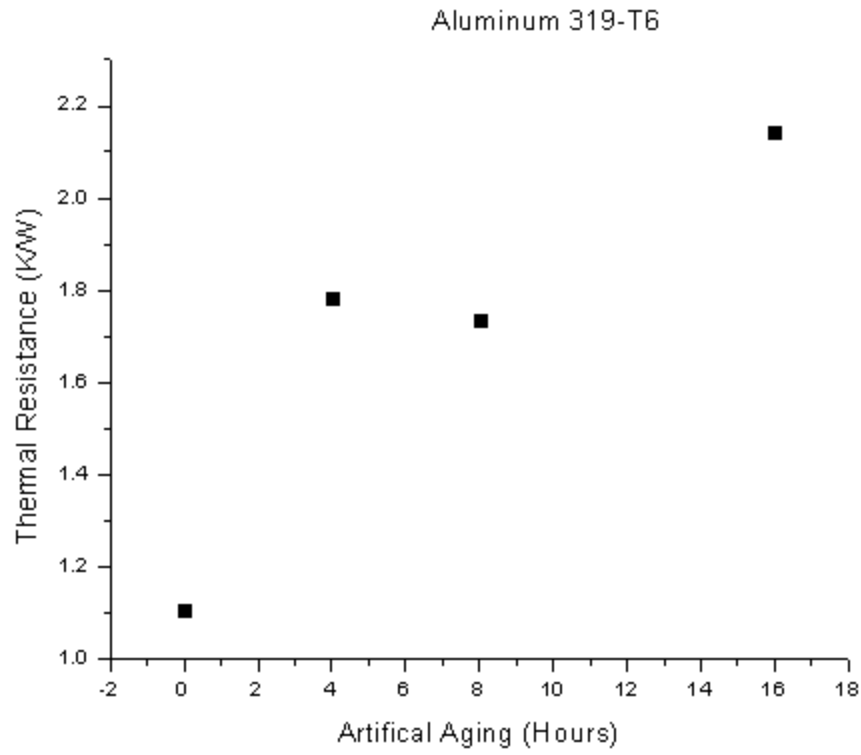


Figure 21: Aluminum 319-T6 thermal resistivity vs artificial aging time length.

5. Highlights & future work

The most interesting point to note is that the thermal resistance increases very rapidly in the beginning stages of artificial aging. To get a more clear understanding of what is going on during the early part of aging would be measure more test samples at very short time lengths of artificial aging.

6. References

- [1] <http://asm.matweb.com/search/SpecificMaterial.asp?bassnum=MA6061t6>
- [2] Alex C. Burr, “Notes on the History of the Concept of Thermal Conductivity”
- [3] ASM International
- [4] <http://www.electronics-cooling.com/2000/05/how-thermal-conductivity-relates-to-electrical-conductivity/>
- [5] <http://ntrs.nasa.gov/archive/nasa/casi.ntrs.nasa.gov/20090032058.pdf>
- [6] <http://prb.aps.org/pdf/PRB/v72/i11/e115120>
- [7] <http://www.thermopedia.com/content/781/>
- [8] Gibson J. W. “Equilibrium diagrams and common metal alloy systems” Kensington, N.S.W. : Clarendon Press, 1977.
- [9] Granta material intelligence CES EduPack

Appendix A

Sample 1

Current	voltage	P_0	DT_raw	DTcorr	errDT	Reff	Rcorr	Raverage
amps	volts	watts	K	K	K	K/W	K/W	
0	0	0	-0.0515	0	0.0224	--		
0.0054	2	0.0108	-0.0211	0.0304	0.0215	2.81481481	0.98765432	0.98417686
0.0111	4	0.0444	0.0781	0.1296	0.0214	2.91891892	1.02418208	
0.0167	6	0.1002	0.2296	0.2811	0.0219	2.80538922	0.9843471	
0.0223	8	0.1784	0.4267	0.4782	0.0221	2.68049327	0.94052396	

Sample 2

Current	voltage	P_0	DT_raw	DTcorr	errDT	Reff	Rcorr	Raverage
amps	volts	watts	K	K	K	K/W	K/W	
0	0	0	-0.0435	0	0.0242	--		
0.0051	2	0.0102	-0.0122	0.0313	0.0212	3.06863	1.07671139	1.08377904
0.0107	4	0.0428	0.0951	0.1386	0.0227	3.23832	1.13625184	
0.0167	6	0.1002	0.2649	0.3084	0.0218	3.07784	1.07994537	
0.0223	8	0.1784	0.4864	0.5299	0.0214	2.97029	1.04220754	

Sample 3

Current	voltage	P_0	DT_raw	DTcorr	errDT	Reff	Rcorr	Raverage
amps	volts	watts	K	K	K	K/W	K/W	
0	0	0	-0.0209	0	0.0258	--		
0.0055	2	0.011	-0.0149	0.006	0.0211	0.54545	0.19138756	0.80962667
0.0112	4	0.0448	0.1033	0.1242	0.0217	2.77232	0.97274436	
0.0169	6	0.1014	0.276	0.2969	0.0219	2.92801	1.02737119	
0.0226	8	0.1808	0.5186	0.5395	0.0217	2.98396	1.04700357	

Sample 4

Current	voltage	P_0	DT_raw	DTcorr	errDT	Reff	Rcorr	Raverage
amps	volts	watts	K	K	K	K/W	K/W	
0	0	0	-0.0377	0	0.0212	--		
0.0055	2	0.011	0.0043	0.042	0.0219	3.81818	1.33971292	1.2112792
0.0111	4	0.0444	0.1156	0.1533	0.0217	3.4527	1.21147463	
0.0168	6	0.1008	0.2993	0.337	0.022	3.34325	1.17307157	
0.0225	8	0.18	0.5373	0.575	0.0218	3.19444	1.1208577	

Sample 5

Current	voltage	P_0	DT_raw	DTcorr	errDT	Reff	Rcorr	Raverage
amps	volts	watts	K	K	K	K/W	K/W	
0	0	0	-0.0376	0	0.0213	--		
0.0054	2	0.0108	-0.0043	0.0333	0.0218	3.08333	1.08187135	0.99273685
0.0111	4	0.0444	0.0891	0.1267	0.0219	2.8536	1.00126442	
0.0167	6	0.1002	0.2356	0.2732	0.0223	2.72655	0.95668312	
0.0222	8	0.1776	0.4337	0.4713	0.0219	2.65372	0.9311285	

Sample 6

Current	voltage	P_0	DT_raw	DTcorr	errDT	Reff	Rcorr	Raverage
amps	volts	watts	K	K	K	K/W	K/W	
0	0	0	-0.0403	0	0.0223	--		
0.0055	2	0.011	-0.0033	0.037	0.0216	3.36364	1.18022329	1.07667915
0.0112	4	0.0448	0.0968	0.1371	0.0214	3.06027	1.0737782	
0.0168	6	0.1008	0.2591	0.2994	0.0219	2.97024	1.04218881	
0.0225	8	0.18	0.4781	0.5184	0.0221	2.88	1.01052632	

Sample 7

Current	voltage	P_0	DT_raw	DTcorr	errDT	Reff	Rcorr	Raverage
amps	volts	watts	K	K	K	K/W	K/W	
0	0	0	-0.0466	0	0.0223	--		
0.0054	2	0.0108	-0.0105	0.0361	0.0219	3.34259	1.17283951	1.08438799
0.0111	4	0.0444	0.0925	0.1391	0.0216	3.13288	1.09925715	
0.0168	6	0.1008	0.2559	0.3025	0.0219	3.00099	1.05297967	
0.0225	8	0.18	0.4728	0.5194	0.022	2.88556	1.01247563	

Sample 8

Current	voltage	P_0	DT_raw	DTcorr	errDT	Reff	Rcorr	Raverage
amps	volts	watts	K	K	K	K/W	K/W	
0	0	0	-0.042	0	0.0209	--		
0.0054	2	0.0108	-0.0036	0.0384	0.0212	3.55556	1.24756335	1.15503442
0.0108	4	0.0432	0.1037	0.1457	0.0214	3.37269	1.18339831	
0.0165	6	0.099	0.2726	0.3146	0.022	3.17778	1.11500975	
0.0222	8	0.1776	0.5017	0.5437	0.0217	3.06137	1.07416627	

Sample 10

Current	voltage	P_0	DT_raw	DTcorr	errDT	Reff	Rcorr	Raverage
amps	volts	watts	K	K	K	K/W	K/W	
0	0	0	-0.0323	0	0.022	--		
0.0054	2	0.0108	0.0183	0.0506	0.0213	4.68519	1.64392463	1.47220548
0.0111	4	0.0444	0.1511	0.1834	0.0222	4.13063	1.44934408	
0.0166	6	0.0996	0.3739	0.4062	0.0222	4.07831	1.43098711	
0.0223	8	0.1784	0.6615	0.6938	0.0222	3.88901	1.36456612	

Appendix B

Sample 1 (2 hours)

Current	voltage	P_0	DT_raw	DTcorr	errDT	Reff	Rcorr	Raverage
amps	volts	watts	K	K	K	K/W	K/W	
0	0	0	-0.0346	0	0.0228	--		
0.0024	2	0.0048	0.0129	0.0475	0.0218	9.89583	3.47222222	1.40314927
0.0052	4	0.0208	0.1704	0.205	0.0225	9.85577	3.45816464	
0.0122	6	0.0732	0.3096	0.3442	0.0265	4.70219	1.64988975	
0.0183	8	0.1464	0.4479	0.4825	0.0276	3.29577	1.15640878	

Sample 2 (4 hours)

Current	voltage	P_0	DT_raw	DTcorr	errDT	Reff	Rcorr	Raverage
amps	volts	watts	K	K	K	K/W	K/W	
0	0	0	-0.0313	0	0.0222	--		
0.003	2	0.006	0.015	0.0463	0.0221	7.71667	2.70760234	1.21253666
0.0067	4	0.0268	0.1711	0.2024	0.0224	7.55224	2.64990835	
0.0133	6	0.0798	0.2647	0.296	0.0229	3.70927	1.30149936	
0.0183	8	0.1464	0.4375	0.4688	0.0231	3.20219	1.12357396	

Sample 3 (8 hours)

Current	voltage	P_0	DT_raw	DTcorr	errDT	Reff	Rcorr	Raverage
amps	volts	watts	K	K	K	K/W	K/W	
0	0	0	-0.037	0	0.0215	--		
0.0025	2	0.005	0.019	0.056	0.0217	11.2	3.92982456	1.43918446
0.0056	4	0.0224	0.1921	0.2291	0.022	10.22768	3.58865915	
0.0138	6	0.0828	0.3116	0.3486	0.0243	4.21014	1.47724383	
0.0184	8	0.1472	0.5508	0.5878	0.0238	3.99321	1.4011251	

Sample 6 (4 hours)

Current	voltage	P_0	DT_raw	DTcorr	errDT	Reff	Rcorr	Raverage
amps	volts	watts	K	K	K	K/W	K/W	
0	0	0	-0.0428	0	0.0217	--		
0.0028	2	0.0056	0.0137	0.0565	0.0228	10.08929	3.54010025	1.78341949
0.0059	4	0.0236	0.1851	0.2279	0.0224	9.65678	3.38834374	
0.0116	6	0.0696	0.3879	0.4307	0.0286	6.18822	2.1713047	
0.0176	8	0.1408	0.5172	0.56	0.0232	3.97727	1.39553429	

Sample 7 (8 hours)

Current	voltage	P_0	DT_raw	DTcorr	errDT	Reff	Rcorr	Raverage
amps	volts	watts	K	K	K	K/W	K/W	
0	0	0	-0.0362	0	0.0225	--		
0.0026	2	0.0052	0.027	0.0632	0.0219	12.15385	4.26450742	1.7367762
0.0053	4	0.0212	0.2081	0.2443	0.0226	11.52358	4.04336312	
0.0113	6	0.0678	0.3856	0.4218	0.0228	6.22124	2.18289086	
0.0192	8	0.1536	0.5288	0.565	0.0224	3.67839	1.29066155	

Sample 8 (16 hours)

Current	voltage	P_0	DT_raw	DTcorr	errDT	Reff	Rcorr	Raverage
amps	volts	watts	K	K	K	K/W	K/W	
0	0	0	-0.044	0	0.0222	--		
0.0026	2	0.0052	0.017	0.061	0.0218	11.73077	4.11605938	2.14154944
0.0053	4	0.0212	0.1892	0.2332	0.0225	11	3.85964912	
0.0081	6	0.0486	0.3583	0.4023	0.0238	8.27778	2.90448343	
0.0185	8	0.148	0.5375	0.5815	0.0249	3.92905	1.37861546	

Appendix C

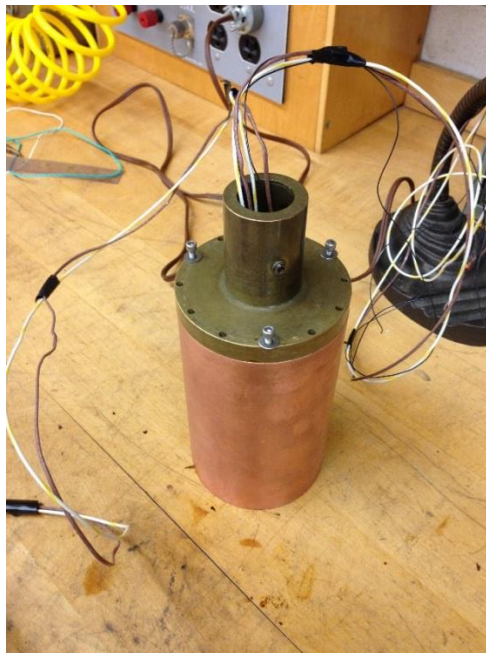
Sample Dimensions

Sample	length(in)	diameter(in)	length(m)	diameter(m)	area(m ²)
1	2.445	0.6355	0.06210300	0.01614170	0.00020464
2	2.431	0.633	0.06174740	0.01607820	0.00020303
3	2.461	0.625	0.06250940	0.01587500	0.00019793
4	2.415	0.635	0.06134100	0.01612900	0.00020432
5	2.434	0.6185	0.06182360	0.01570990	0.00019384
6	2.363	0.63	0.06002020	0.01600200	0.00020111
7	2.335	0.631	0.05930900	0.01602740	0.00020175
8	2.393	0.631	0.06078220	0.01602740	0.00020175
9	2.128	0.632	0.05405120	0.01605280	0.00020239
10	2.3	0.638	0.05842000	0.01620520	0.00020625

Copper Calibration Sample

Current amps	voltage volts	P_0 watts	DT_raw K	DTcorr K	errDT K	Reff K/W	Rcorr K/W	Raverage
0	0	0	-0.0376	0	0.022	--		
0.0026	2	0.0052	-0.0029	0.0347	0.0225	6.67308	2.3414305	0.80102461
0.0055	4	0.022	0.0674	0.105	0.0218	4.77273	1.67464115	
0.0166	6	0.0996	0.1921	0.2297	0.022	2.30622	0.80920172	
0.0221	8	0.1768	0.3619	0.3995	0.0218	2.25962	0.7928475	

Apparatus



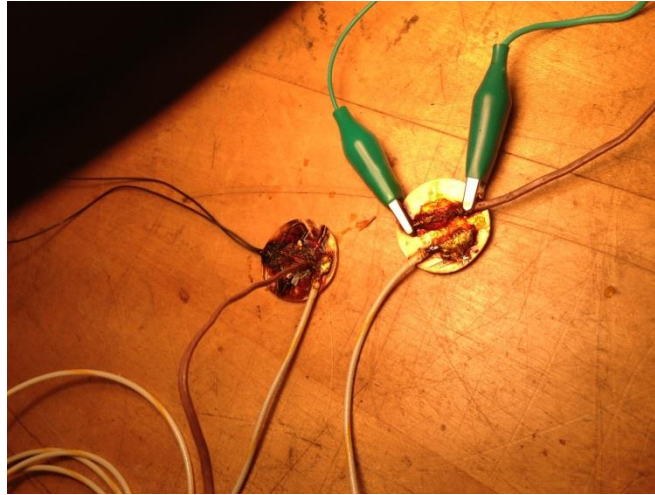
Removable inner structure




Apparatus hooked up and inside larger tank



Attachments with GE Varnish on the copper connection plates



Presentation Poster



WPI

Thermal and Electrical Transport

Advisors: Germano S. Innacchione and Diana A. Lados

1. Abstract

The goal of this project was to design, build, and validate a high-resolution apparatus to measure thermal and electrical property changes in heat treatable aluminum alloys. These property changes were caused by the formation and growth of precipitates during the artificial aging stage of the heat treatment. In-situ and ex-situ experiments were designed for two precipitation strengthened aluminum alloys (wrought 6061 and cast 319) to capture and quantify changes in both thermal and electrical conductivity. Measurements were made at different stages during the artificial aging process to understand the effects of precipitates size and distribution on the resulting transport properties of the materials. A comparison of the results from the in-situ and ex-situ experiments was also performed. The selected alloys will also indicate differences in thermal and electrical properties due to the presence of secondary phases (conic; in particular). The developments and findings in this study will be presented and discussed.

2. Design and Construction

The overall goals of the design specifications and manufacturing are as follows:

- Create an outside container that would have a high heat inertia to have a steady temperature controlled environment for the samples.
- Obtain with a high copper content was used for the water container (Figure 2) based on its high heat capacity.
- Create a removable inner structure that can be easily removed to change samples and have very low thermal and electrical conductivity.
- Teflon pieces and Pvcex tubing were used to build the inner structure (Figure 3), can be disconnected easily.
- Create circuit for a 1-dimensional flow of heat transfer.
- Pvcex tubing was used to enclose the sample with minimal heat taken away from the samples.
- Have a circular connection plate that has very high thermal and electrical conductivity to send most of the power to the sample.
- This copper plate (relative to a potting) were used based on the very high thermal and electrical conductivity. These copper connection plates were sandblasted and polished to create a very flat finish for good thermal contact.

3. Experimental Setup

The two copper connection plates are tightly clamped together by the Teflon screws. The bottom copper connection plate has a strain gage (used as a heater, a thermocouple or thermometer), and an electrical lead to apply voltage. The top copper connection plate has a thermocouple and an electrical lead attached. A power supply, multimeter, and thermocouple were utilized.








Figure 1. Solidworks design of apparatus. Figure 2. Full construction. Figure 3. Removable inner structure that changes the samples between the two copper connection plates.

4. Samples Tested

There are five aluminum 6061 samples and five aluminum 319 samples. These aluminum alloys were chosen to be tested based on industry use and the heat treatability of the two. Aluminum 6061 is used in aircraft and aerospace components. Both Aluminum 6061 and aluminum 319 are used in the automotive industry in high heat applications (increasing the aging process) including cylinder heads and engine blocks. Determining the effects of precipitates on thermal and electrical conductivity is sought from these materials.

Aluminum Alloy	Solution heat treatment (temp, time)	Quench	Artificial aging		Testing Measurements
			Temperature (°C)	Time (hr)	
6061-1	500, 24	water	150	16, 32, 48	Electrical conductivity, thermal conductivity, strain gage
6061-2	500, 24	water	150	16, 32, 48	Electrical conductivity, thermal conductivity, strain gage
6061-3	500, 24	water	150	16, 32, 48	Electrical conductivity, thermal conductivity, strain gage
6061-4	500, 24	water	150	16, 32, 48	Electrical conductivity, thermal conductivity, strain gage
6061-5	500, 24	water	150	16, 32, 48	Electrical conductivity, thermal conductivity, strain gage
319-1	500, 24	water	150	16, 32, 48	Electrical conductivity, thermal conductivity, strain gage
319-2	500, 24	water	150	16, 32, 48	Electrical conductivity, thermal conductivity, strain gage
319-3	500, 24	water	150	16, 32, 48	Electrical conductivity, thermal conductivity, strain gage
319-4	500, 24	water	150	16, 32, 48	Electrical conductivity, thermal conductivity, strain gage
319-5	500, 24	water	150	16, 32, 48	Electrical conductivity, thermal conductivity, strain gage

5. Methodology

- 1) The inner structure is set up by having a sample placed into the Pvcex tube and enclosed by the Teflon screws. The copper connection plates are tightly clamped the sample by the Teflon screws.
- 2) The inner structure is then placed into the water container, then the test container is placed into a hot tank.
- 3) Once the thermocouple readings are at equilibrium with the water temperature data was noted to be logged (page 4).
- 4) The voltage to the strain gage heater was applied at 2 volts. Once the two thermocouples equilibrate with the heat addition, the voltage was increased to 4 volts, then 6 volts, then 8 volts.

To determine the thermal conductivity k , equation (1) below was used. With the known cross-sectional area and length, as well as the calculated heat flow Q , the thermal conductivity can be found.

$$k = \frac{Q \cdot L}{A \cdot \Delta T} \quad (1)$$

Thermal Conductivity = heat \cdot length / (area \cdot temperature gradient)

The electrical conductivity is defined as the inverse of electrical resistivity. To determine the electrical conductivity in equation (2) below was used. With the length and cross-sectional area known, as well as the measured electrical resistance R , the electrical conductivity can be found.

$$\sigma = \frac{L}{R \cdot A} \quad (2)$$

Electrical Conductivity = electrical resistivity \cdot area \cdot length

6. Results

The apparatus had a noise of $\pm 0.1^\circ\text{C}$. The temperature readings were stable but in the large water container used in Figure 4 the heat pump in comparison are due to the resistance in cooling to the main page at 2, 4, 6, and 8 volts. The blue line represents the bottom copper connection plate and the green represents the top copper connection plate.

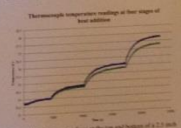


Figure 4. Temperature readings on the top and bottom of a 2.2 inch Aluminum 6061 rod.

7. Acknowledgements

Ryan W. Smith
Xiang Chen
Instituto de Investigaciones

38